Mon. Not. R. astr. Soc. (1987) **224,** 131–154

Antenna patterns of interferometric detectors of gravitational waves – I. Linearly polarized waves

Bernard F. Schutz and Massimo Tinto *Department of Applied Mathematics and Astronomy, University College, PO Box 78, Cardiff CF1 1XL*

Accepted 1986 July 18. Received 1986 April 2

Summary. We consider the response of a free-mass interferometric gravitational wave detector to plane gravitational waves arriving from an arbitrary direction with an arbitrary linear polarization in the long-wavelength approximation. After deriving the well-known single-detector antenna pattern η, we address the problem of a detector fixed on the Earth observing gravitational wave bursts that arrive from the direction of the Virgo cluster with random polarization and random arrival time.

First we calculate the rms sensitivity of a single detector $\langle \eta^2 \rangle^{1/2}$ as a function of its latitude and orientation on Earth. Then we consider coincidences between two fixed detectors. Let each detector have a threshold X, being the minimum detectable value of η^2. The coincidence probability C clearly depends upon the thresholds X_1 and X_2 of the two detectors. However, we are able to prove a remarkable result for random burst of gravitational waves, that the mean squared product of the antenna patterns $\langle \eta_1^2 \eta_2^2 \rangle$ equals the average of the coincidence probability of the two detectors over all thresholds,

$$\int_0^1 \int_0^1 C(X_{1*}, X_{2*})\, dX_{1*}, dX_{2*}.$$

It is therefore possible to extract meaningful information about coincidences from the purely geometrical function $\langle \eta_1^2 \eta_2^2 \rangle$. We argue that this function probably underestimates realistic coincidence probabilities, but does so uniformly, so it allows comparisons to be made between different sites and different orientations at the same site. By plotting this function for several pairs of likely detector locations in the USA and Europe for random waves from Virgo, we find a number of interesting results, among which are: (i) coincidences between detectors in the USA are very sensitive to small changes in their relative orientations, and (ii) the coincidence probability between a detector in the USA and one in Europe is generally a factor of about 2 smaller than probabilities within America or Europe. We also perform similar calculations for sources randomly distributed on the sky. Finally, we discuss the implications of these results for the choice of orientation of the planned detectors and for the numbers of detectors world-wide.

1 Introduction

Experiments aimed at the detection of gravitational waves, in which changes in the relative motions of three or more widely separated and nearly free test masses are monitored using laser interferometers, are now being developed in several laboratories.

The experiments will be sensitive to kilohertz-frequency waves, which are expected to come from supernovae and other stellar-mass collapse events, the richest nearby source of which is the Virgo cluster. The detectors will be large (arm lengths of several kilometres) and expensive, and therefore there are likely to be few of them ($\leqslant 5$ in the world in this century). Once a detector is built, it will be difficult to move it or even to change its orientation. These detectors have a quadrupolar antenna pattern, so their location and orientation on Earth affect their sensitivity to gravitational wave bursts and especially the likelihood of detections of the same event by two or more detectors. Coincident detections of bursts are crucial, not only in giving more confidence in the reality of the event but also in providing directional information from the time delays between detectors. On the other hand, because events may be rare (less than once a month), directional antennas miss valuable data. Accordingly, in this paper we study the effect that a detector's location has on its sensitivity, and the effect that the latitudes, relative longitudes and orientations of two detectors have on the probability of coincident detections. We find that for relatively close detectors, such as two in North America, the coincidence probability is rather sensitive to the orientation of the antennas' arms relative to the local compass directions, while for one detector in America and another in Europe, the coincidence probability is rather lower. It is nevertheless possible to find consistent orientations for American and European detectors that simultaneously maximize all their coincidence probabilities. Whether this is desirable is something we will discuss below.

In Fig. 1 we have schematically represented an interferometric detector as a central mass (labelled 1) and two others (2 and 3) some distance l_0 away in perpendicular directions, all of them freely suspended and acting as free particles in the horizontal plane in their response to an incident gravitational wave. For a complete physical description of such a detector we refer the reader to the fundamental papers by Drever (1982) and Weiss (1979). While we have drawn the arms perpendicular to each other, detectors with 60° included angle have been discussed (Maischberger *et al.* 1985), and we will accordingly allow for such detectors in this paper.

The response of such a detector consists basically of the change δl in the relative length of the two arms (we shall be more precise below). The size of this response depends on a number of factors:

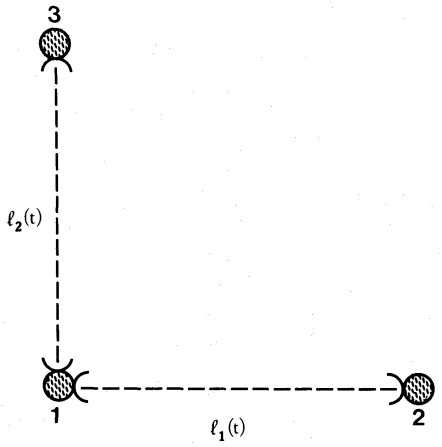

Figure 1. Schematic diagram of a three-mass interferometric gravity-wave detector.

(1) The dimensionless amplitude h, polarization and waveform of the incoming gravitational waves. The response is linear in h. The gravitational wave bursts should be unpolarized. Continuous wave-sources such as pulsars usually emit circularly polarized radiation. First-generation detectors will probably be sensitive only to bursts dominated by kilohertz frequencies, but later improvements may allow the study of lower frequencies, e.g. for waves from pulsars.

(2) The orientation of the detector with respect to the direction of travel of the wave and the opening angle 2Ω between the arms. Detectors are linearly polarized and gravitational waves are transverse. Their relative orientation is determined by the detector's situation on Earth, by the location of the source on the sky, and by the time of arrival of the signal (since the detectors are carried by the Earth's rotation). We shall refer to these as the geometrical factors affecting the detector's response.

(3) The level of noise in the detector and its statistical distribution. In practice a variety of noise sources will set an effective minimum δl_* on the measurable response δl. We shall make the convenient but somewhat naïve assumption that any δl larger than δl_* is detected and any smaller one is lost.

Our aim is to study the geometrical factors in a detector's response. Once a detector is sited, its location and geographical orientation are difficult to change, whereas factors affecting the noise limits on sensitivity will be continually changed by the experimenters. Other factors are random or out of the experimenter's control: the amplitude, polarization, and time of arrival of the waves. Continuous-wave sources will be local and therefore distributed over the sky. Burst sources can be detected at larger distances, so we will at first assume that they are predominantly in the Virgo cluster, although we will see that this does not affect our conclusions much.

We give here a short summary of our methods and conclusions. In Section 2 we study the response of a single detector to a wave of arbitrary polarization and direction of source, working in the long-wavelength approximation (reduced wavelength $\lambda/2\pi \gg$ arm length l_0). The *antenna pattern* of the detector, as defined as

$$\eta = \frac{\delta l}{h l_0}, \tag{1.1}$$

depends only on the source and polarization angles relative to the detector's axes, and has a maximum value of 1. (If the detector arms make an angle 2Ω, the maximum is $\sin 2\Omega$.) It will be the quantity of most interest to us. In Section 3 we convert this expression to one giving η as a function of the location and orientation of the detector on Earth, the polarization and source position in the sky and the time of arrival of the wave. By fixing the source in the Virgo cluster and averaging over random polarizations and times of arrival, we find the rms value of η as a function of the detector's latitude and orientation. (The longitude of the detector disappears when we average over times of arrival!) This allows one to estimate the fraction of events with detectable amplitudes which a detector will miss because of unfavourable geometrical factors. In Section 4 we turn to coincidence observations with two detectors whose antenna patterns are called η_1 and η_2. Without specifying a threshold sensitivity for each detector it is impossible to calculate a coincidence probability, but in the spirit of this paper we wish to consider only the geometrical factors. A threshold-independent measure of the relation between η_1 and η_2 is the correlation coefficient

$$\varrho \equiv \frac{\langle \eta_1 \eta_2 \rangle}{\langle \eta_1^2 \rangle^{1/2} \langle \eta_2^2 \rangle^{1/2}}$$

of the amplitudes, where angle brackets denote averages over random polarization and arrival times. This is relatively easy to calculate but it is unfortunately unsatisfactory, since it is linear in η_1 and η_2: an event giving large values of η_1 and η_2 of opposite sign would be regarded by observers as a coincident detection, but such events tend to reduce the value of ϱ. We therefore consider the antenna's *power pattern*

$$X=\eta^2, \tag{1.2}$$

and compute the mean overlap of the power patterns

$$F_{12}=\langle X_1X_2\rangle. \tag{1.3}$$

We show, in fact, that there is a closer relationship between F_{12} and the probabilities of coincidences that one might have expected. Let $C(X_{1*}, X_{2*})$ be the probability that if detector 1 and detector 2 have thresholds X_{1*} and X_{2*} respectively (having values between 0 and 1), then they will both be triggered by events randomly distributed in polarization and arrival time. Then we show that:

$$\langle X_1X_2\rangle=\int_0^1\int_0^1 C(X_{1*}, X_{2*})\,dX_{1*}\,dX_{2*}. \tag{1.4}$$

Thus we may regard $\langle X_1X_2\rangle$ as the mean of the coincidence probability over all thresholds.

The calculation of F_{12} was performed in the algebraic computing language MACSYMA, and required considerable machine resources. We shall only display it for selected values of its arguments. In particular we fix the locations of the detectors and plot F_{12} as a function of their orientations. We do this only for detectors located in Nevada, Maine, Scotland and Southern Germany. These are at present the most likely sites for first-generation detectors.

We conclude Section 4 with a discussion of the mean coincidence probabilities for randomly-distributed burst sources. Here all pairs of detectors have a mean coincidence probability considerably higher than for Virgo sources. In Section 5 we discuss the results.

2 Single-detector response function

Since all the likely sources of gravitational waves are very far away from the Earth, the signal we hope to detect will have a very small amplitude and can be considered a plane wave. This allows us to study the problem by using the linearized version of Einstein's field equations, which are derived in most serious textbooks (e.g. Misner, Thorne & Wheeler 1973). In particular, defining the metric perturbation $h_{\mu\nu}$ and its trace-reverse $\bar{h}_{\mu\nu}$ by

$$g_{\mu\nu}=n_{\mu\nu}+h_{\mu\nu}, \qquad \bar{h}_{\mu\nu}=h_{\mu\nu}-\tfrac{1}{2}n_{\mu\nu}h_{\alpha\beta}n^{\alpha\beta}, \tag{2.1}$$

with $n_{\mu\nu}$ the Minkowski metric and $|h_{\mu\nu}|\ll 1$, then Einstein's equations may be written as follows, where $\Box=\nabla^2-\partial^2/\partial t^2$:

$$\left.\begin{aligned}&\Box\bar{h}_{\theta\nu}=0\\&n^{\alpha\beta}\bar{h}_{\mu\alpha,\beta}=0\end{aligned}\right\}. \tag{2.2}$$

Assuming we work in T.T. gauge (see Misner *et al.* 1973), $\bar{h}_{\mu\nu}$ becomes (in matrix form and for a wave propagating in the Z direction

$$\bar{h}_{\mu\nu}(\text{T.T.})=\begin{bmatrix}0&0&0&0\\0&h_+&h_\times\exp(i\delta)&0\\0&h_\times\exp(i\delta)&-h_+&0\\0&0&0&0\end{bmatrix}\exp[i(\omega t-kZ)] \tag{2.3}$$

(see Misner *et al.* 1973 or Schutz 1985). The coefficients h_+ and $h_\times$ are the amplitudes of the two independent polarizations.

To work out the detector's response δl we shall use the equation of geodesic deviation (see, for its derivation, Schutz 1985)

$$\frac{d^2\xi^\alpha}{d\tau^2}=R^\alpha_{\beta\gamma\delta}U^\beta U^\gamma\xi^\delta, \tag{2.4}$$

where U^β is the tangent vector field to a given geodesic congruence, ξ^α is the connecting vector field of the congruence and $R^\alpha_{\beta\gamma\delta}$ is the Riemann tensor for the given Levi-Civita connection. We may use this equation only if the distance ξ^α is significantly smaller than a wavelength. In our case only the geodesics associated with the three test masses 1, 2 and 3 are of interest. In our coordinates the components of U^β are needed only to lowest order [any corrections to U^β depend on $h_{\alpha\beta}$, and will give higher order contributions to equation (2.4)].

Therefore we can assume

$$U^\beta=\delta^\beta_0. \tag{2.5}$$

Taking into account (2.5) in (2.4) we have

$$\frac{d^2\xi^\alpha}{dt^2}=R^\alpha_{00\beta}\xi^\beta. \tag{2.6}$$

In particular it is easy to prove that (see Schutz 1985)

$$R^0_{00\beta}=0 \tag{2.7}$$

$$R^K_{00R}=-\tfrac{1}{2}\bar{h}^{K(\mathrm{T.T.})}_{R,00} \tag{2.8}$$

where Greek indices run from 0 to 3 and Latin indices from 1 to 3.

Now let us introduce orthogonal Cartesian coordinates x, y, z such that the x–y plane contains our detector and (somewhat unconventionally) the x-axis bisects the angle 2Ω between the detectors' arms (Fig. 2). This arrangement is the most convenient one for our later discussion of coincidences. Next we introduce another three coordinates X, Y, Z with the plane gravitational wave. Z is parallel to the propagation direction of the wave and X and Y are the axes of the

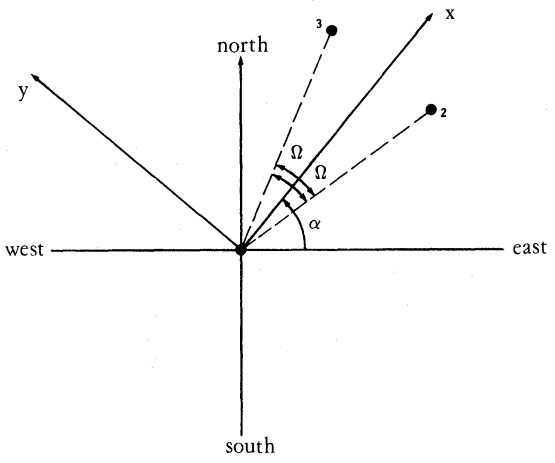

Figure 2. The relationships of the detector's arms (dashed lines making an angle 2Ω), the detector's x–y axes (with the x-axis bisecting the angle between the arms), and the local compass directions (defining the angle α that we will use later).

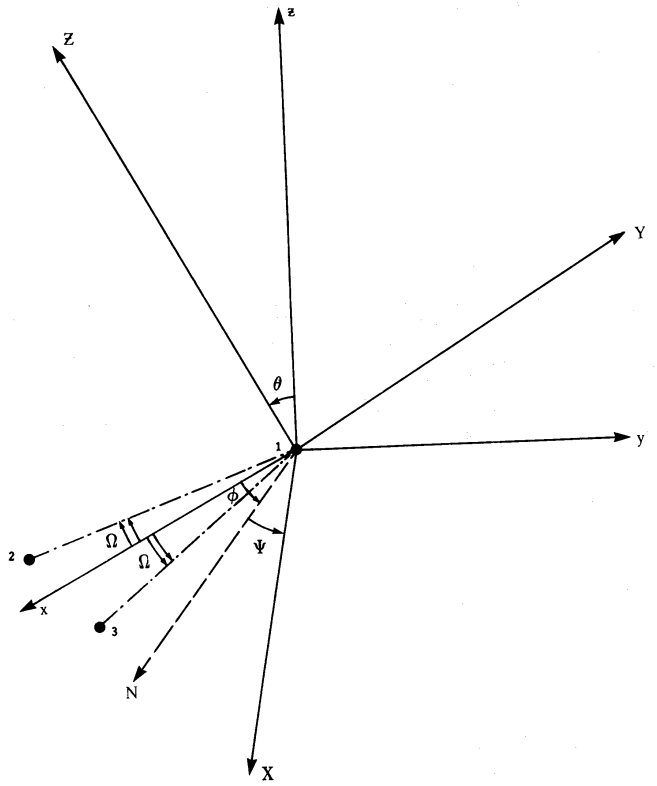

Figure 3. The relation between the detector's axes (x, y, z) and the wave's axes (X, Y, Z). The angles θ and ϕ are the usual spherical polar coordinates of the wave's direction of travel as measured in the detector's frame. The angle ψ is a measure of the polarization angle of the wave; it represents a rotation about the Z-axis. The line N is the line of nodes, not the local north.

polarization ellipse of the wave. In Fig. 3 we introduce the usual Eulerian angles θ, ϕ, ψ [where θ and ϕ give the incoming direction of the wave and ψ is the angle between one semi-axis of the ellipse of polarization wave and the node direction N (see Goldstein 1965)].

Since the experiment is performed in the (x, y, z) coordinates (the detector's frame of reference), it is necessary to introduce explicitly the orthogonal matrix transformation from (X, Y, Z) to (x, y, z)

$$(A)^j_K = \begin{bmatrix} \cos\psi\cos\phi - \cos\theta\sin\phi\sin\psi, & -(\sin\psi\cos\phi + \cos\theta\sin\phi\cos\psi), & \sin\theta\sin\phi \\ \cos\psi\sin\phi + \cos\theta\cos\phi\sin\psi, & -\sin\psi\sin\phi + \cos\theta\cos\phi\cos\psi, & -\sin\theta\cos\phi \\ \sin\theta\sin\psi, & \sin\theta\cos\psi, & \cos\theta \end{bmatrix}$$

where we have adopted the convention [already used in (2.8)] of using capital Latin letters for the frame (X, Y, Z) and lower case for (x, y, z).

From equations (2.6), (2.7) and (2.8) one deduces that

$$\frac{d^2\xi^K}{dt^2} = -\tfrac{1}{2} h^{K(\mathrm{T.T.})}_{R,00}\xi^R, \tag{2.10}$$

and from equation (2.9), for the orthogonal transformation A, we have

$$\xi^i = A^i_R\xi^R \quad \text{and} \quad \xi^K = (A^t)^K_j\xi^j.$$

Consequently from (2.10) we easily get

$$\frac{d^2\xi^i}{dt^2}=-\tfrac{1}{2}A^i_R\bar{h}^{R(\mathrm{T.T.})}_{K,00}(A^t)^K_j\xi^j. \tag{2.11}$$

At the order of h we are working with, we can assume $\xi^i(t)\cong\xi^i(0)$ on the right side of (2.11) since any corrections to ξ^i depend on h_{ij} and will give higher order contributions to (2.11). The Fourier components of (2.11) in the band of frequencies of interest therefore obey the equation

$$\delta\xi^i=-\tfrac{1}{2}A^i_R\bar{h}^{R(\mathrm{T.T.})}_{K}(A^t)^K_j\xi^j(0). \tag{2.12}$$

The change in length of any one arm is easily found in terms of the unit vector n_i parallel to it

$$\delta l_n/l_0=-\tfrac{1}{2}[(A^i_XA^j_X-A^i_YA^j_Y)h_+ +(A^i_XA^j_Y-A^j_XA^j_Y)\exp(i\delta)h_\times]n_in_j. \tag{2.13}$$

The quantity measured by the interferometer is δl, the difference between the values of δl_n for the two arms. Given that the arms have unit vectors $(\cos\Omega, -\sin\Omega, 0)$ and $(\cos\Omega, \sin\Omega, 0)$, we find

$$\delta l/l_0=-\sin 2\Omega[(A^x_XA^y_X-A^x_YA^y_Y)h_+ +(A^x_XA^y_Y+A^x_YA^y_X)\exp(i\delta)h_\times]. \tag{2.14}$$

Let us consider two extreme cases for the gravitational waves:

(i) If the waves are linearly polarized then without loss of generality we may take $h_+=h>0$ and $h_\times=0$. Then (2.14) becomes

$$\delta l=\sin 2\Omega[\cos 2\phi\sin 2\psi\cos\theta+\tfrac{1}{2}(1+\cos^2\theta)\sin 2\phi\cos 2\psi]l_0h. \tag{2.15}$$

This is equivalent to expressions already obtained by others (e.g. Estabrook 1985, Weiss (unpublished) and Forward 1978), when account is taken where necessary of the different orientation of the x–y axes with respect to the detector's arms that we have adopted.

(ii) Circularly polarized gravitational waves. In this case, let us assume $h_+=h_\times=h>0$ and $\delta=\pi/2$ in (2.3). Equation (2.14) is rewritten as:

$$\delta l=[\tfrac{1}{2}\sin 2\phi(1+\cos^2\theta)+i\cos 2\phi\cos\theta]\exp(-2i\psi)hl_0\sin(2\Omega). \tag{2.16}$$

Notice that (2.15) and (2.16) are periodic in ϕ and ψ with period π, and in fact δl just changes sign as either angle increases by $\pi/2$. This reflects the quadrupolar nature of the detector (ϕ) and the polarization of the wave (ψ).

In Fig. 4 we have plotted contours of equal value of $\delta l/hl_0$ for a linearly polarized gravitational wave having $\psi=0°$. Not surprisingly, the antenna pattern attains local maxima for $\theta=0°$, 180° and $\phi=45°$, 135°, i.e. when the wave is incident normal to the plane of the arms with the same polarization as the detector. When $\phi=0°$, 90° our function is identically equal to zero, independently of θ. Physically this is due to the fact that the vibration direction of the wave makes equal angles with the detector's two arms in the plane (x, y) and therefore implies $\delta l_1=\delta l_2$.

In Fig. 5 we have considered again a linearly polarized gravitational wave with $\psi=45°$. From the figure we see that at $\theta=90°$ (wave incident in the plane of the detector) our function is identically equal to zero, for all ϕ values (for all direction in this plane) and, at the same time, when $\phi=45°$, 135° (i.e. when the wave is incident in the plane containing one arm of the detector and perpendicular to the other), it is zero for all θ values. The explanation of these facts is again clear from symmetry arguments. The maximum value for $\psi=45°$ is reached when $\theta=0°$, 180° and $\phi=0°$, 90°, which is physically the same configuration as the maximum in the case $\psi=0°$: a wave incident normally to the detector's plane and with the same polarization as the detector.

Finally, in Fig. 6 we have plotted $|\delta l|/l_0h$, from (2.16), for a circularly polarized gravitational wave. As we may see, our function has two zeros: $\theta=90°$, $\phi=0°$ and 90°. At $\theta=0°$, 180°, it is constant and equal to 1 because the gravitational wave's plane and that of the detector coincide. It

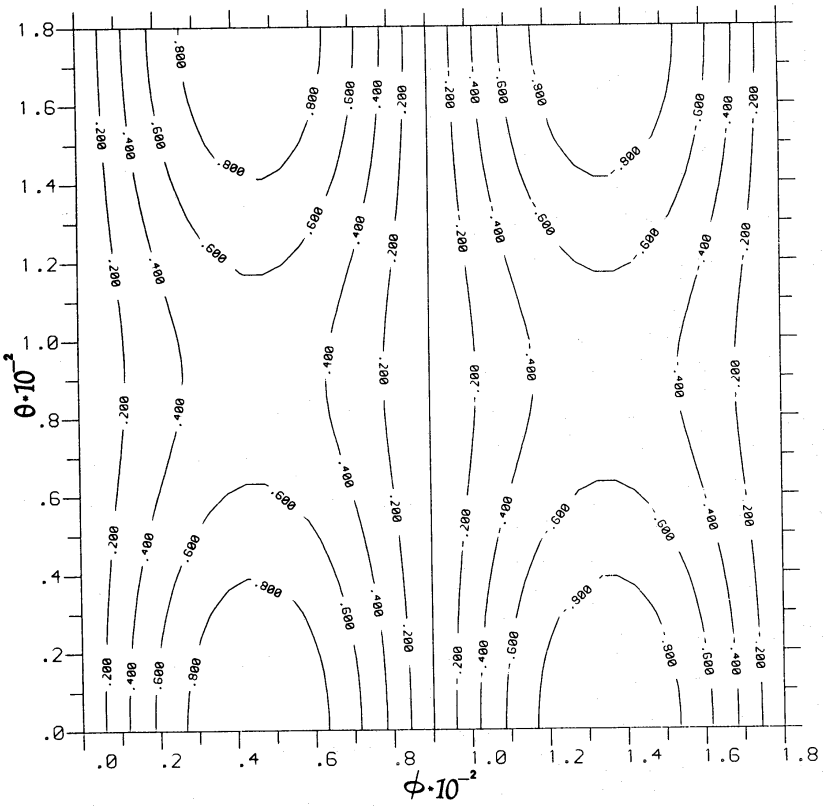

Figure 4. Contours of the antenna pattern η defined in (1.1) for a wave having linear polarization, $\psi=0°$, as given by (2.5). The angles are as in Fig. 3.

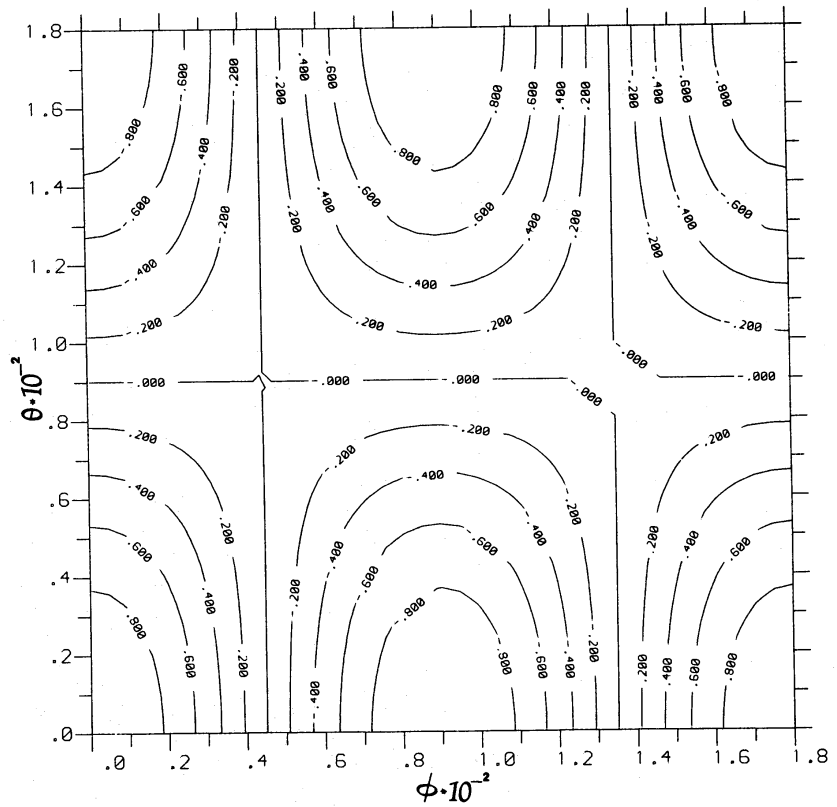

Figure 5. As Fig. 4 with $\psi=45°$.

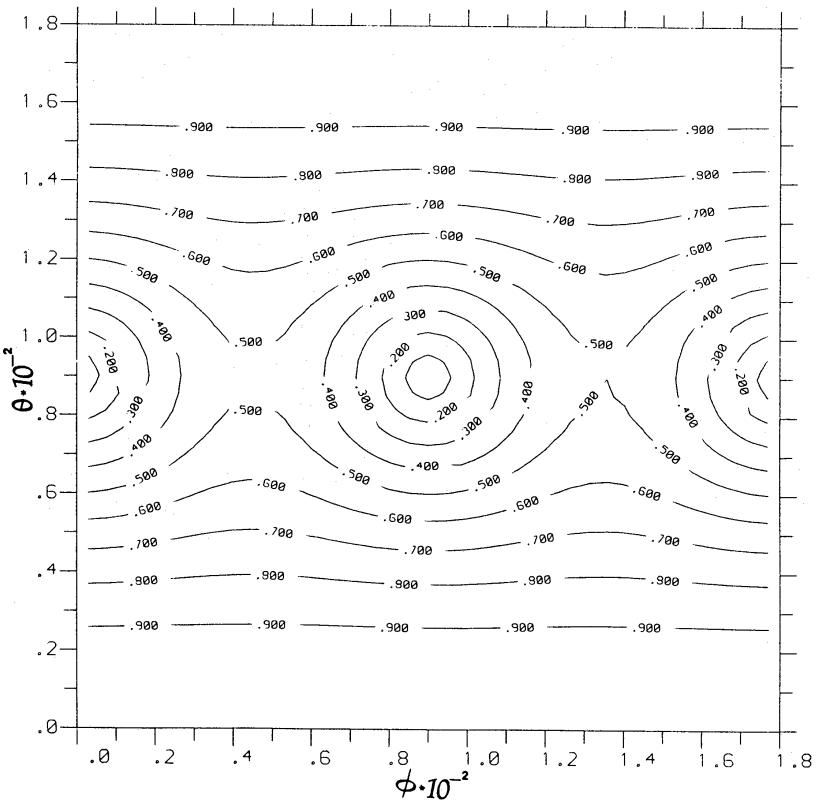

Figure 6. The modulus $|\eta|$ for a circularly polarized wave.

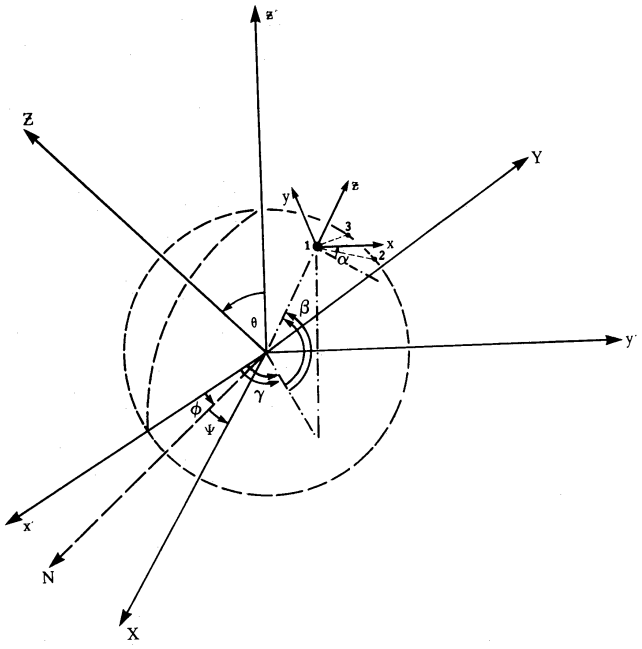

Figure 7. The relations among the detector's axes (x, y, z), the Earth's axes (x', y', z') and the wave's axes (X, Y, Z). Here β and γ are the detector's latitude and longitude, respectively, and α its orientation as in Fig. 2. As in Fig. 5, the angles θ and ϕ give the incoming direction of the wave, but here this is measured with respect to the Earth's axes. Again, the angle ψ determines the polarization angle of the wave. Since ϕ and γ are angles in the same (x', y') plane, only $\phi-\gamma$ is relevant to the wave-detector interaction.

is important to observe that the function $|\delta l|/hl_0$ for a circularly polarized gravitational wave is exactly twice the square root of the function $\delta l^2/h^2 l_0^2$ of a linearly polarized gravitational wave, averaged on the polarization angle ψ. For simplicity we shall limit our attention only to linearly polarized gravitational waves. We will return to elliptical polarization in a future paper.

3 Response of a detector as a function of position on Earth

Now we introduce a third set of coordinates to allow us to place our detector in a given position on the Earth, at latitude β, longitude γ and with its bisector making an angle α with the local meridian (see Fig. 7).

In Fig. 7 the angles (θ, ϕ, ψ) are the Euler angles of the orthogonal transformation from the previous axes (X, Y, Z), associated to the gravitational wave, to the orthogonal axes (x', y', z') centred in the Earth and having the z'-axis parallel to the Earth's rotation axis; from now on they will be referred to as the Earth's axes. If we define A to be the orthogonal transformation from (X, Y, Z) to (x', y', z'),

$$A\colon (X, Y, Z) \rightarrow (x', y', z'),$$

and B the transformation from (x', y', z') to (x, y, z):

$$B\colon (x', y', z') \rightarrow (x, y, z),$$

then we deduce

$$C = B \cdot A\colon (X, Y, Z) \rightarrow (x, y, z).$$

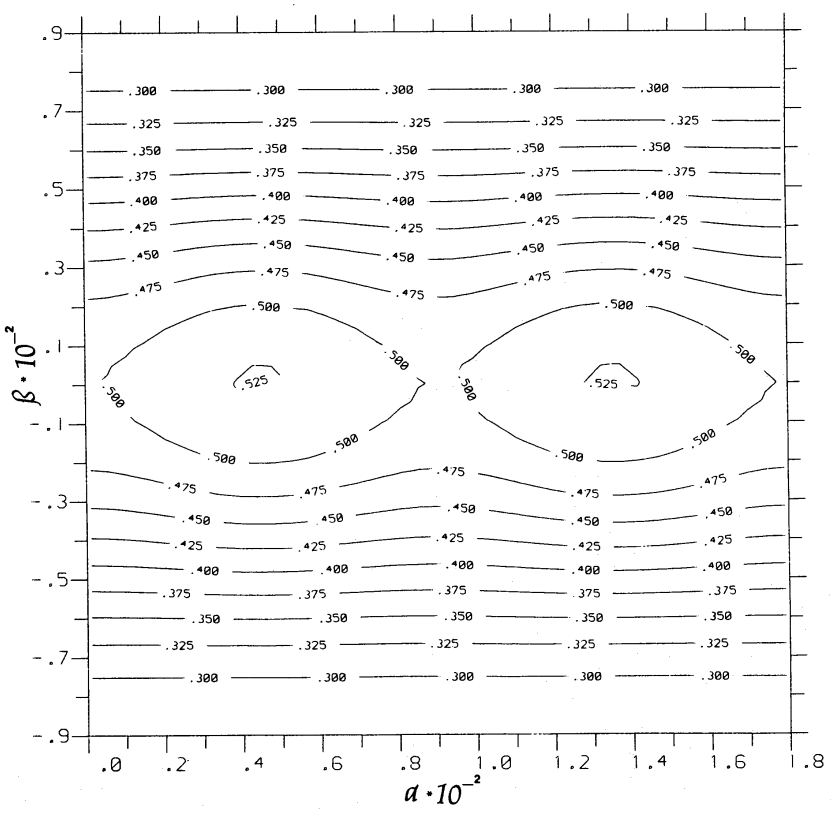

Figure 8. The rms antenna power $\langle X \rangle^{1/2}$ for waves coming from the centre of Virgo ($\theta = 102°$), averaged over arrival times and polarizations, expressed as a function of the latitude β and orientation α of the detector. Above $\pm 40°$ latitude the curves are insensitive to orientation.

We take the angles in A to be the same as before.

The explicit form of B is obtained from A^t by replacements

$\phi \to \gamma - 3\pi/2$, $\psi \to \alpha - \pi/2$ and $\theta \to \pi/2 - \beta$:

$$B = \begin{bmatrix} \cos\alpha \sin\beta \cos\gamma - \sin\alpha \sin\gamma, & \sin\alpha \cos\gamma + \cos\alpha \sin\beta \sin\gamma, & -\cos\alpha \cos\beta \\ -(\cos\alpha \sin\gamma + \sin\alpha \sin\beta \cos\gamma), & -\sin\alpha \sin\beta \sin\gamma + \cos\alpha \cos\gamma, & \sin\alpha \cos\beta \\ \cos\beta \cos\gamma, & \cos\beta \sin\gamma, & \sin\beta \end{bmatrix}.$$

The expression for δl is the same as (2.14) with A replaced by $C = B \cdot A$, and the C^j_K are now functions of $\alpha, \beta, \theta, \psi$, and $(\gamma - \phi)$. Without any loss of generality we can take $\gamma = 0$ for a single detector, replacing changes in longitude by changes in the direction of the incoming wave. Because we average on the angle ψ we shall assume

$h_\times = 0$, $h_+ = h > 0$,

and consequently we have

$$\eta = \delta l / l_0 h = \sin 2\Omega (C^x_X C^y_X - C^x_Y C^y_Y). \tag{3.1}$$

Over a large number of observations we can expect the time of arrival and polarization of the gravitational waves to be random. We therefore take the angles ϕ and ψ to be random variables uniformly distributed on the interval $(0, 2\pi)$ and evaluate the following expectation value

$$\langle X \rangle^{1/2} = \left\langle \left(\frac{\delta l}{l_0 h} \right)^2 \right\rangle^{1/2} \equiv F(\alpha, \beta. \theta). \tag{3.2}$$

We note that, trivially,

$$\langle \eta \rangle = \left\langle \frac{\delta l}{l_0 h} \right\rangle = 0. \tag{3.3}$$

Using MACSYMA on the University College, Cardiff Honeywell DPS-8/70 M we have calculated the function $F(\alpha, \beta, \theta)$ for the special case of waves arriving from the Virgo cluster, for which

$\theta = 102°$

for the incoming plane gravitational wave.

In Fig. 8, we have plotted contours of equal values of the angular function $F(\alpha, \beta, 102°)$ for a fully open detector, $2\Omega = 90°$. (We remind the reader that α and β are respectively the orientation and the latitude of the detector.) In particular we observe that the function is perfectly symmetric with respect to the equatorial plane. This is because two detectors with the same orientation α and at opposite latitudes β and $-\beta$ will assume symmetrical positions with respect to the direction to Virgo at times 12 hr apart.

The maximum value of the sensitivity is at $\beta = 0$ (on the Earth's equator) and at the + orientation with respect to the Earth's coordinates, that is $\alpha = 45°$, $135°$. Going towards higher latitudes, our function smoothly decreases; above a latitude of 40° it is very insensitive to the orientation angle α. In Figs 9 and 10 we have plotted the same angular function evaluated at $\theta = 96°$ and $108°$ respectively, which correspond to sources on the fringes of Virgo. At the middle latitudes at which the first detectors will be built, the antenna power patterns do not differ significantly for these different source directions. Accordingly, in our discussion of coincident observations in the next section we will take all sources in Virgo to be at $\theta = 102°$.

What information about detectors do Figs 8–10 contain? The values of the rms antenna power are to be compared with the maximum value attainable when the wave and antenna are optimally

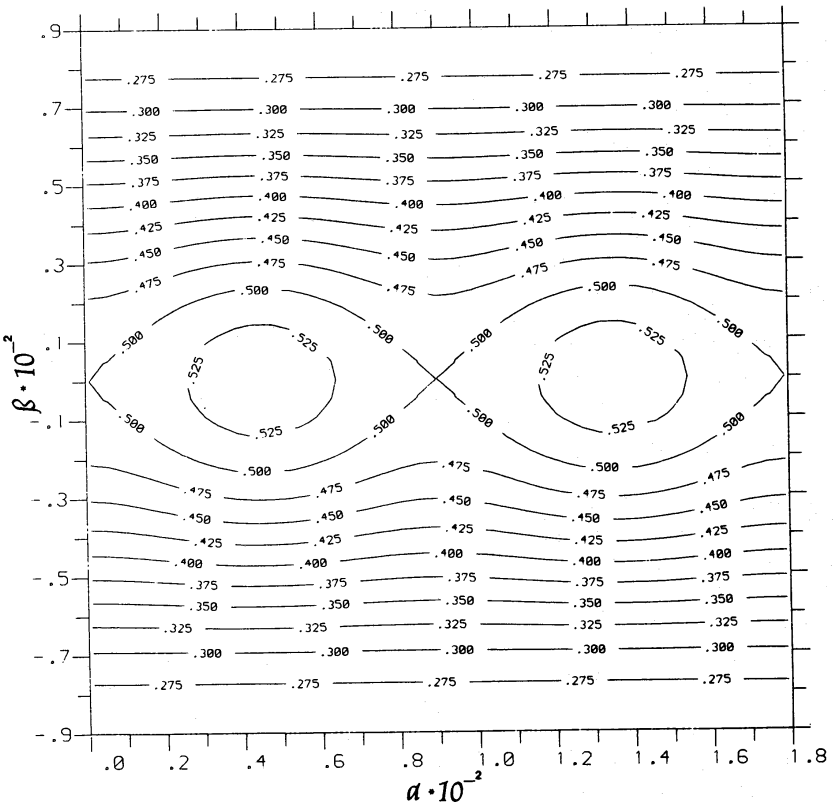

Figure 9. As Fig. 8 for θ=96°, for sources on the fringe of Virgo. Above ±30° latitude there is little change from Fig. 7.

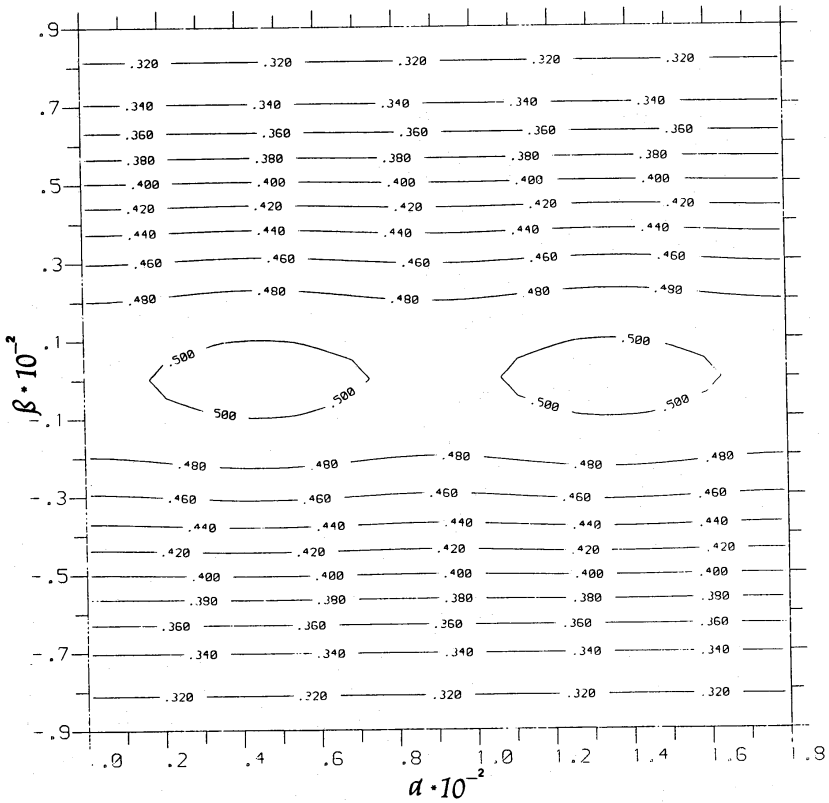

Figure 10. As Fig. 8 for θ=108°, for sources on the other edge of Virgo. Again there is little change above ±30° latitude.

aligned, which is 1. Thus a detector at 45° (New England) will have on average about 40 per cent of its optimum response to gravitational waves of a given amplitude. Put another way, such a detector will have a good chance of detecting only those events that arrive with an intrinsic amplitude h that is two and a half times as large as the detector's threshold.

To use these figures for detectors with acute opening angles 2Ω, all values should be multiplied by $\sin 2\Omega$. Conclusions about relative sensitivity are unaffected.

If sources are isotropically distributed on the sky, then an antenna's location and orientation do not affect its sensitivity. The value of $\langle X\rangle$ averaged over ψ, ϕ and θ (with θ weighted by $\sin\theta$, of course) gives an rms sensitivity

$$\langle X\rangle^{1/2}_{\psi,\phi,\theta}=\frac{1}{\sqrt{5}}=0.447. \tag{3.4}$$

So a detector in the latitudes 30°–50° is about as sensitive to isotropic sources as to Virgo sources with the same amplitude at the Earth.

4 Coincidence experiments

4.1 COINCIDENCE AND CORRELATION FUNCTIONS

Independent detections of any given gravitational wave event by different detectors is vital for its reliable identification as a gravitational wave. This is because the events may not be much larger than the noise level. In Gaussian noise a 5σ excursion will be likely once in every 7×10^5 sampling times. For a kilohertz detector the sample time is of the order of a millisecond, so 5σ events occur five times an hour. Real gravitational wave bursts occur once a month or so, and may not be more than 5σ in amplitude for the first detectors. Independent detectors on the same site provide one way of increasing signal-to-noise, but the extra signal from another detector located elsewhere will probably also be necessary. Moreover, from the time difference between the two detections one can infer a circle on the sky from which the event must have come.

As we remarked earlier, the probability of coincident observations of a given event depends not only on the geometrical factors (overlap of antenna patterns) but also on the thresholds of the detectors relative to the amplitude of the wave. We will now show that there is a remarkably simple relationship between the geometrical factors and the mean of the coincident probability over all the thresholds. Suppose that gravitational wave events, of a given amplitude h and from a fixed location in space (e.g. Virgo), are distributed in arrival time (or apparent hour angle ϕ) and polarization angle ψ with a probability distribution $p(\phi,\psi)$. Then the mean antenna power pattern of antenna 1 is

$$\langle X_1\rangle=\int_0^{2\pi}\int_0^{2\pi}X_1(\phi,\psi)p(\phi,\psi)\,d\phi\,d\psi \tag{4.1}$$

and similarly for antenna 2. This is the square of what we have plotted in Figs 7–9, assuming $p=1/4\pi^2$. Let X_{1*} be the threshold of the squared amplitude, the minimum detectable value of $(\delta l_1/hl_0)^2$. The single-antenna detection probability for a given h is

$$S_1(X_{1*})=\int_{X_1>X_{1*}}p(\phi,\psi)\,d\phi\,d\psi, \tag{4.2}$$

where the integral is over the region of ϕ–ψ space in which X_1 exceeds X_{1*}. The coincidence probability is

$$C(X_{1*},X_{2*})=\int_{\substack{X_1>X_{1*}\\X_2>X_{2*}}}p(\phi,\psi)\,d\phi\,d\psi. \tag{4.3}$$

Now consider the mean of the product of the antenna power functions:

$$\langle X_1X_2\rangle=\int X_1(\phi,\psi)X_2(\phi,\psi)p(\phi,\psi)\,d\phi\,d\psi. \tag{4.4}$$

Let us change variables of integration to X_1 and X_2 themselves. Denoting the Jacobian of that transformation by

$$J=\partial(\phi,\psi)/\partial(X_1,X_2), \tag{4.5}$$

we can write (4.4) as

$$\langle X_1X_2\rangle=\int_0^1\int_0^1 X_1X_2p|J|\,dX_1\,dX_2. \tag{4.6}$$

The limits of integration are the extreme values that X can take. Now we integrate this by parts on X_1 to get

$$\langle X_1X_2\rangle=\int_0^1 X_2\left[-\left(X_1\int_{X_1}^1 p|J|\,d\bar{X}_1\right)_{X_1=0}^{X_1=1}+\int_0^1\left(\int_{X_1}^1 p|J|\,d\bar{X}_1\right)dX_1\right]dX_2. \tag{4.7}$$

The integrated terms vanishes at both limits. After a similar integration on X_2 and a change of notation $X_1\rightarrow X_{1*}$, $\bar{X}_1\rightarrow X_1$ (and similarly for X_2) we obtain:

$$\langle X_1X_2\rangle=\int_0^1\int_0^1\left(\int_{X_{1*}}^1\int_{X_{1*}}^1 p|J|\,dX_1\,dX_2\right)dX_{1*}\,dX_{2*}.$$

By comparison with (4.3), we can see that this is

$$F_{12}=\langle X_1X_2\rangle=\int_0^1\int_0^1 C(X_{1*},X_{2*})\,dX_{1*}\,dX_{2*}. \tag{4.8}$$

Thus, the mean overlap of the antenna power patterns $\langle X_1X_2\rangle$ is the same as the average coincidence probability, i.e. averaged over all possible thresholds X_{1*} and X_{2*}. Given that detector thresholds are likely to change with time, it is not unreasonable to be guided by $\langle X_1X_2\rangle$ when choosing a site for an antenna.

4.2 INTERPRETATION OF THE MEAN COINCIDENCE PROBABILITY

In Figs 11 and 12 we plot contours of constant $\langle X_1X_2\rangle$ for a number of pairs of detectors. The values of $\langle X_1X_2\rangle$ are typically 3–6 per cent, which might suggest that the probability of a coincidence between two detectors is very small. This is not correct, however. The coincidence probability depends on the thresholds X_{1*} and X_{2*}: thresholds near zero mean that the signal is strong relative to the noise level, and it will therefore be detectable almost regardless of what direction it comes from. Thresholds near 1, on the other hand, mean that the signal is relatively weak, and it will be detectable only in a narrow range of incoming directions and polarizations. So thresholds near 1 have low coincidence probabilities. Now consider the averaging over thresholds in (4.8). The integral is over a unit square in X_{1*}–X_{2*} space. Current detector design anticipates that X_* will be less than 0.25 for bursts of amplitude $h=10^{-21}$. For such a case, expected thresholds will be in the sixteenth of the square nearest the origin, where coincidence probabilities are highest. The average in (4.8) therefore weights low coincidence probabilities too strongly for this (hopefully realistic) case.

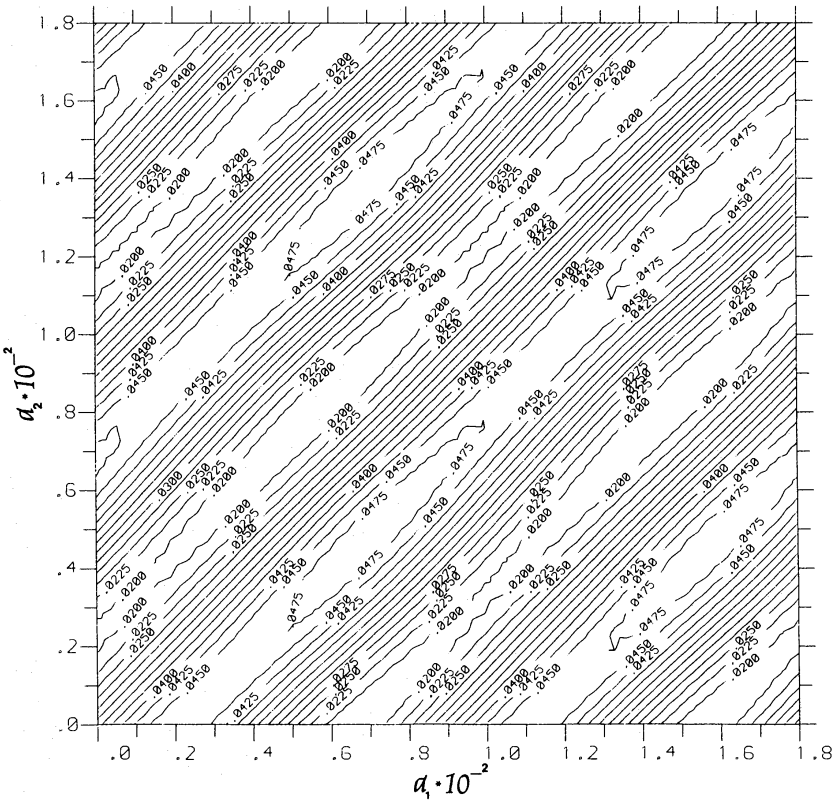

(a)

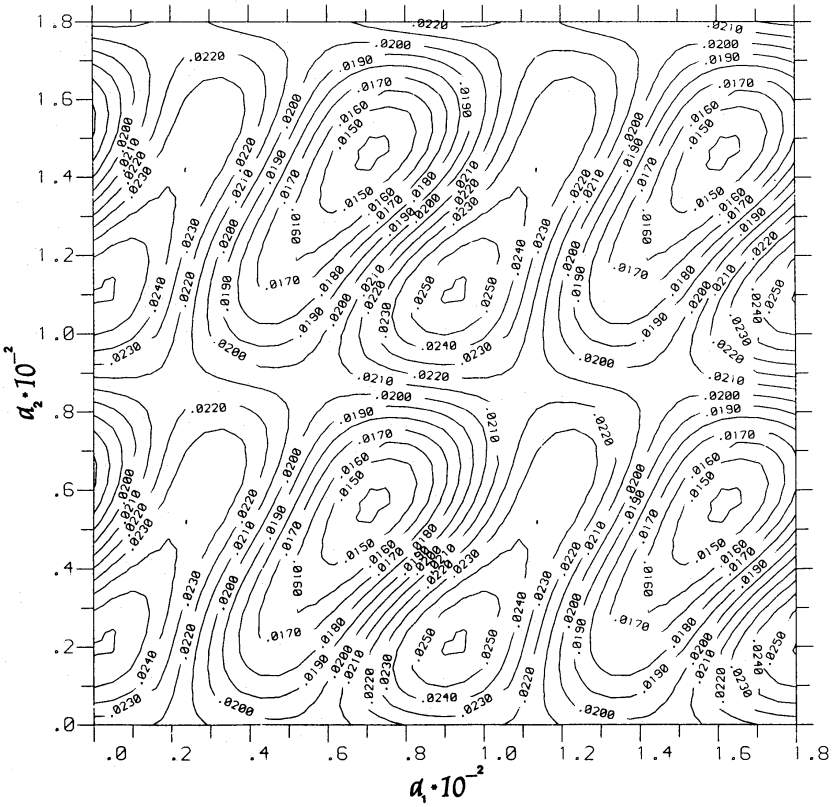

(b)

Figure 11. (a)–(f) display contours of constant $\langle X_1 X_2 \rangle$ as functions of the orientations of various pairs of detectors, for sources in Virgo. See the text for a full discussion.

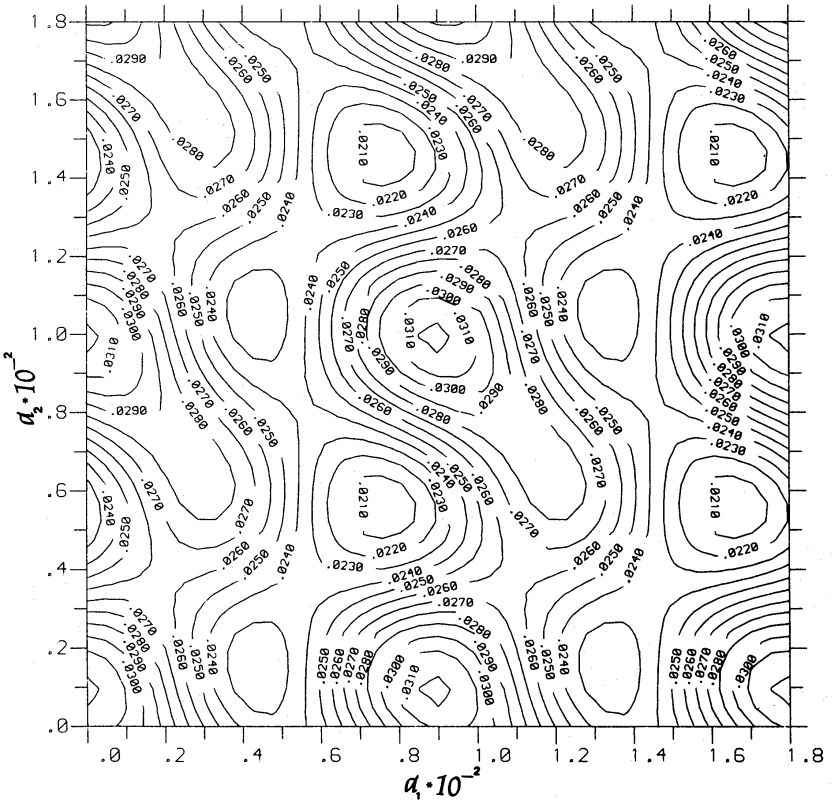

(c)

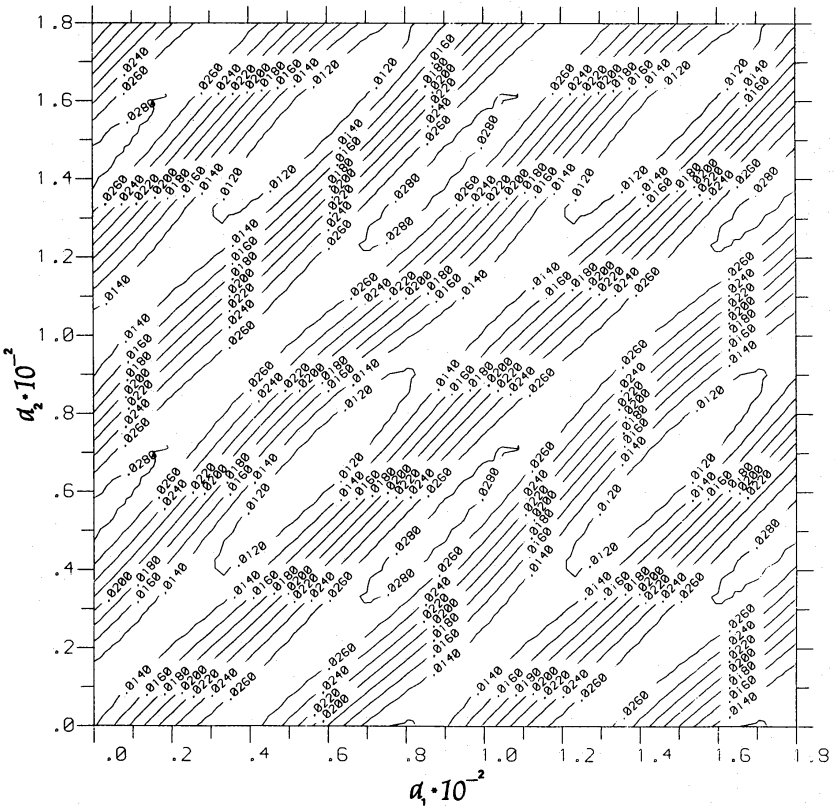

(d)

Figure 11 – *continued*

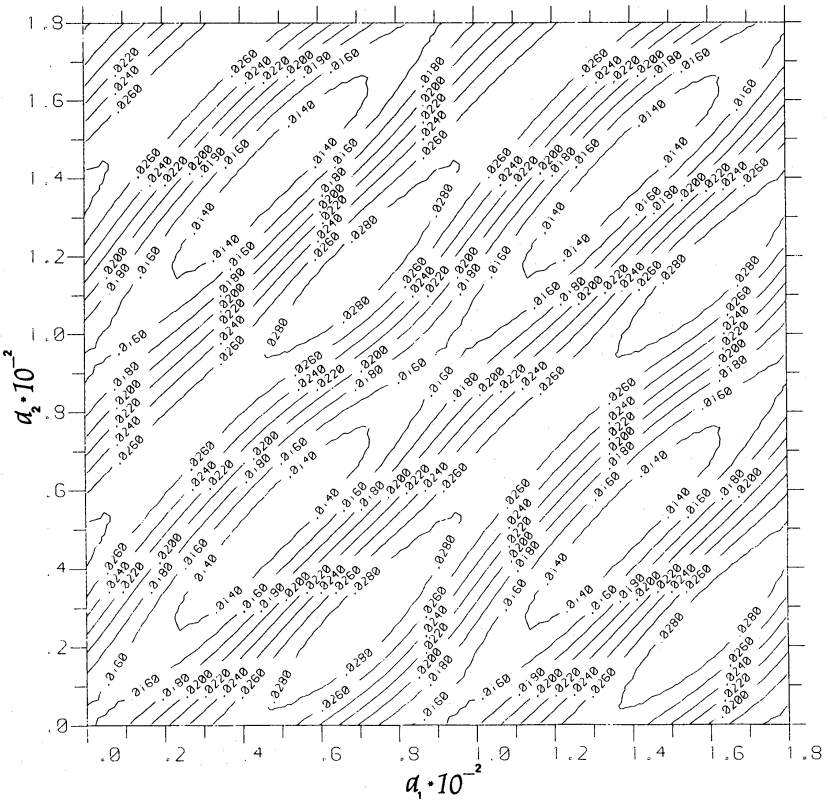

(e)

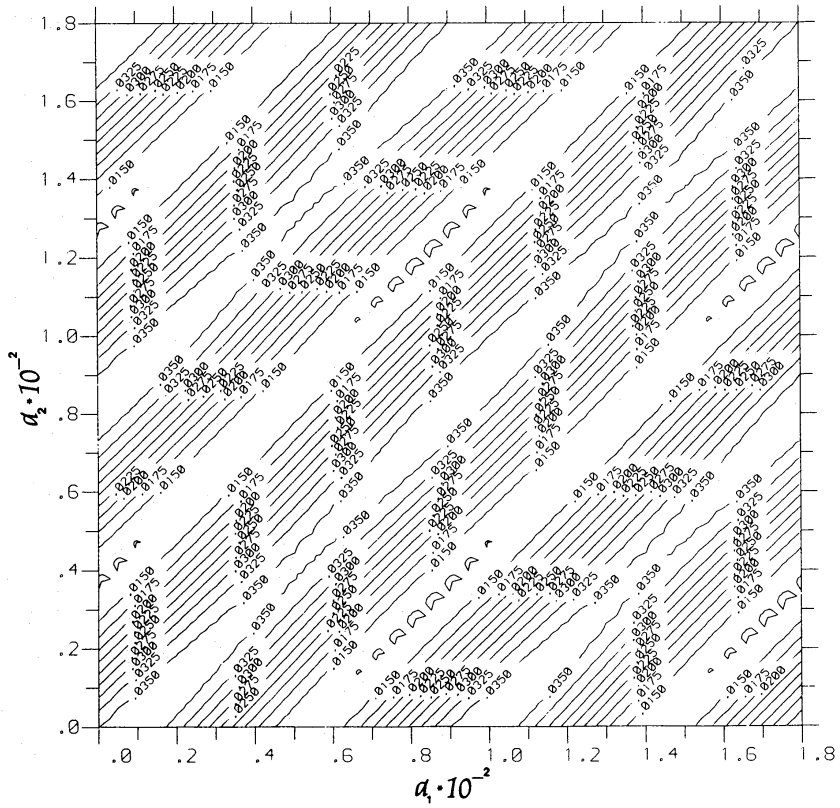

(f)

Figure 11 – *continued*

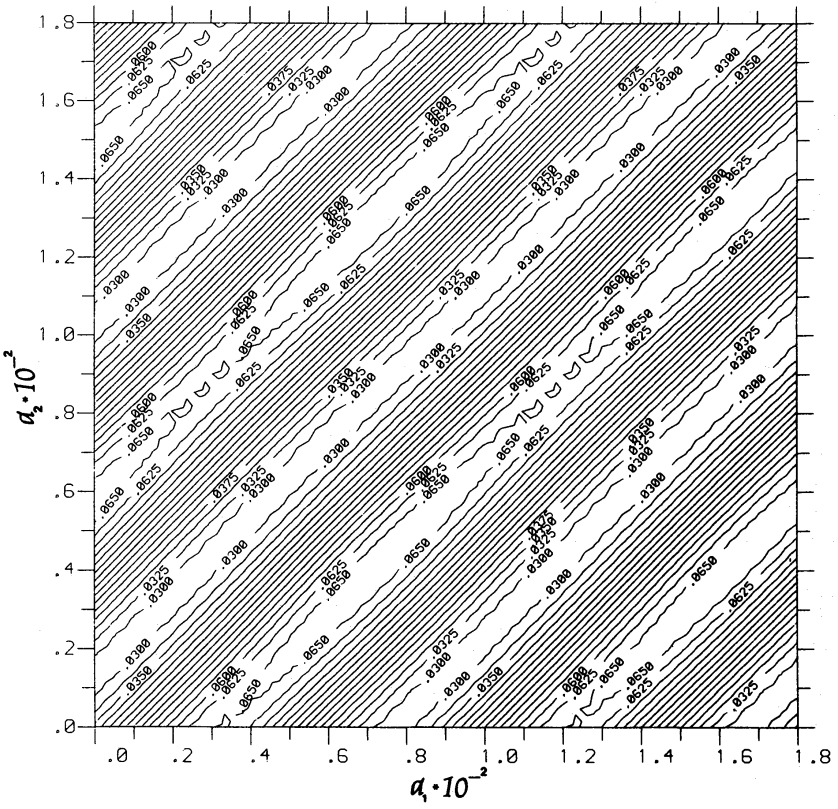

(a)

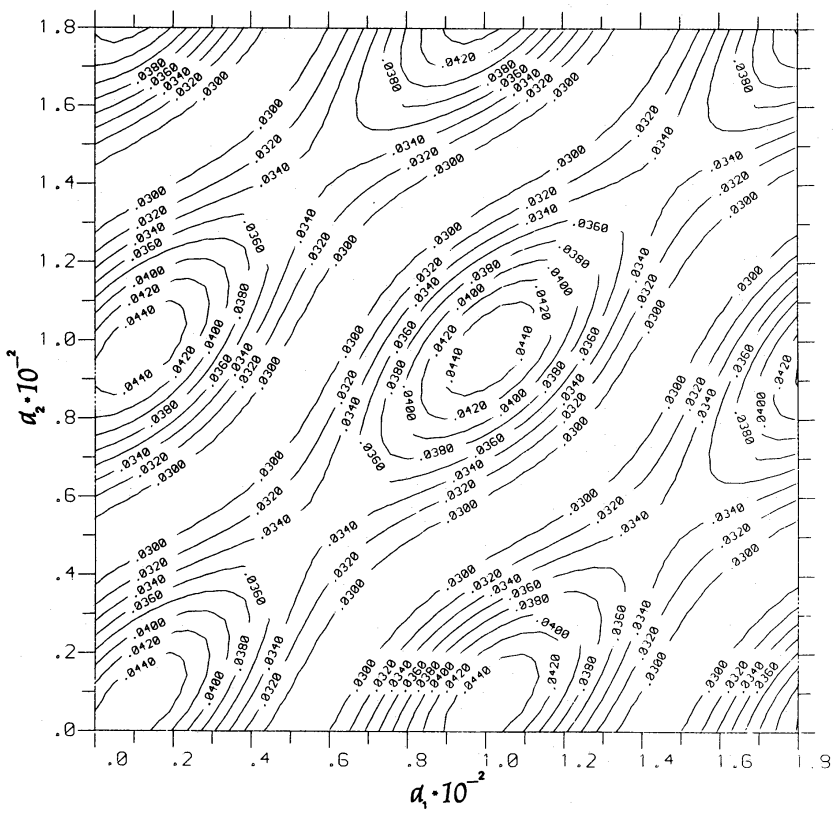

(b)

Figure 12. As Fig. 11 but for sources isotropically distributed on the sky.

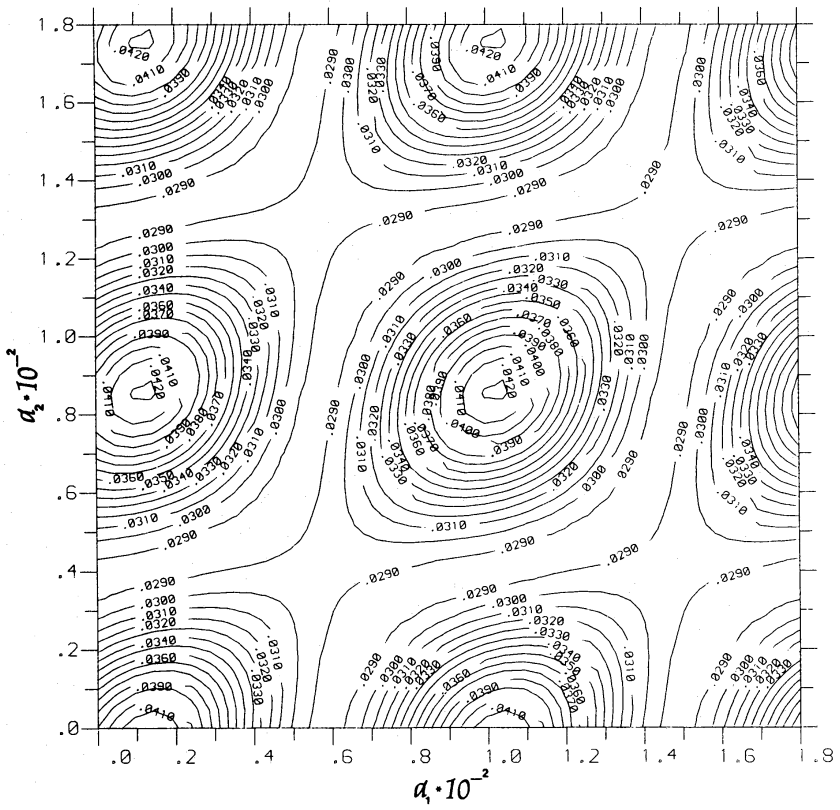

(c)

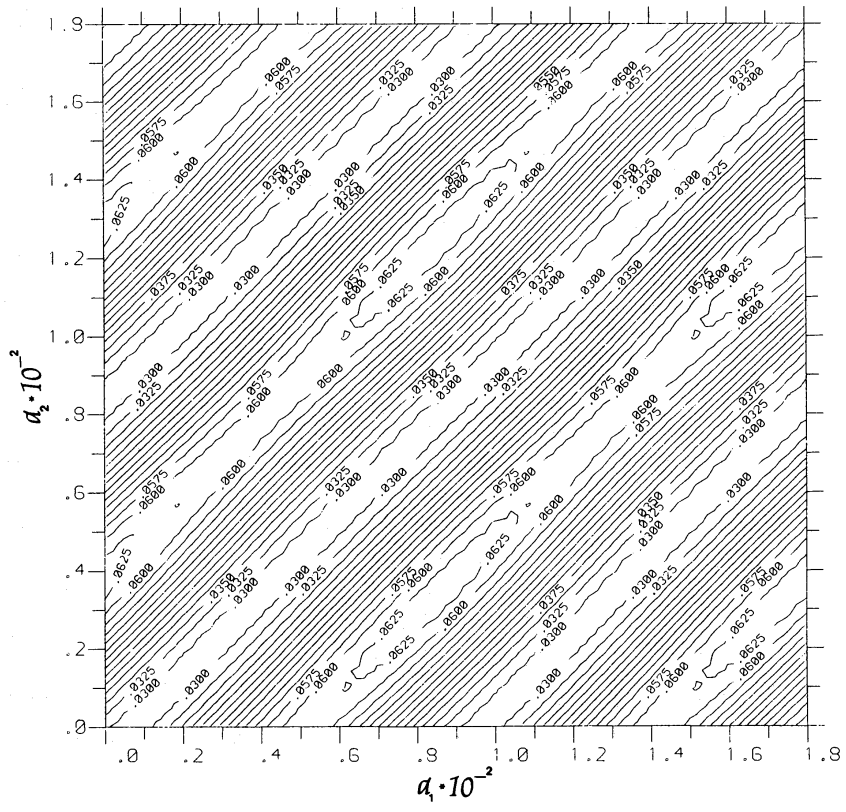

(d)

Figure 12–*continued*

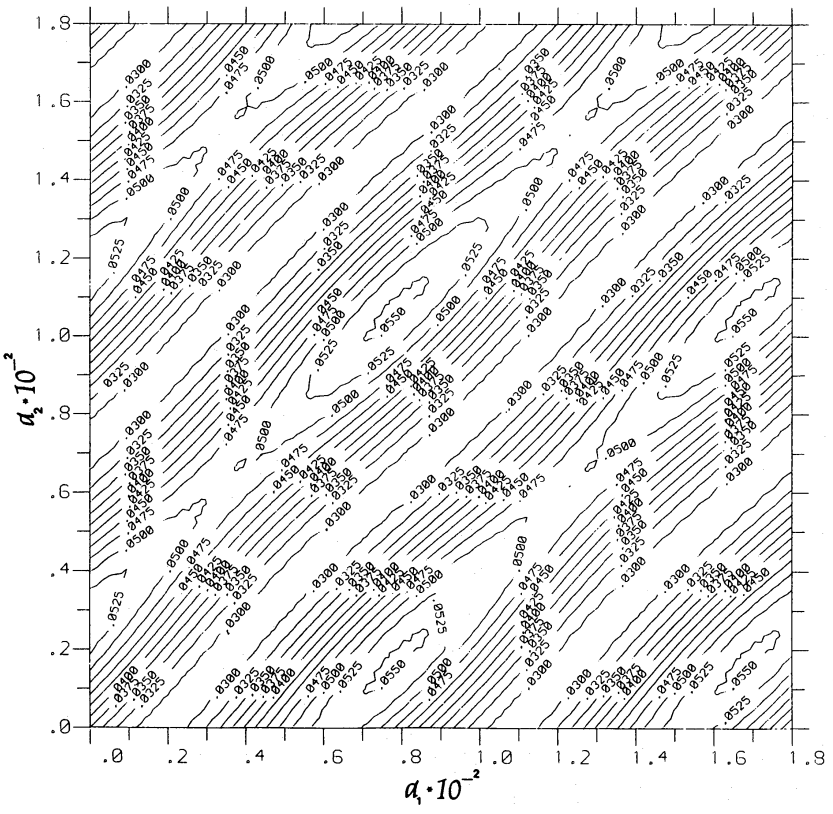

(e)

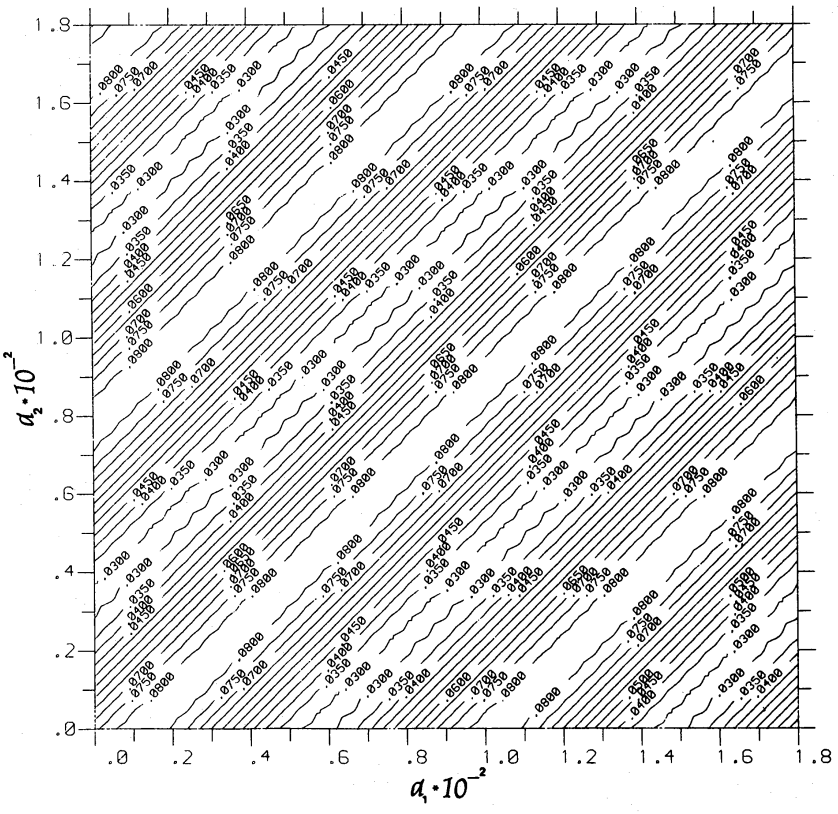

(f)

Figure 12–*continued*

By how much does $\langle X_1X_2\rangle$ underestimate the expected coincidence probability? A full answer to this requires a calculation of actual coincidence probabilities, which we plan for a subsequent paper. But here we can do a simple calculatation that will give us some idea of how to scale $\langle X_1X_2\rangle$ to make it more realistic. Consider two identical antennas next to each other, on the equator, both in the '+' orientation, and receiving bursts from a source directly above the equator. In this case the coincidence probability is the same as the signal-detector detection probability, which can be found from (2.15). As the Earth turns, the source scans through θ for $\phi=45°$, and its polarization ψ is random. So the coincidence probability is the fraction of θ–ψ space in which $|\delta l/l_0h|^2>X_*$. For $X_*=0.25$, it is not hard to calculate that this is 47 per cent. On the other hand, the value of $\langle X_1X_2\rangle$ is the mean value of $|\delta l/l_0h|^4$ over the same space, which is 16 per cent. So in this case $\langle X_1X_2\rangle$ underestimates the coincidence probability for $X_*=0.5$ by a factor of 3. Now, more realistic pairs of antennas have lower coincidence probabilities, but this is due to the geometrical factors that $\langle X_1X_2\rangle$ is sensitive to. We believe, therefore, that for any pair of antennas the mean coincidence probability is probably about a factor of 3 smaller than the true coincidence probability for $X_{1*}=X_{2*}=0.5$. On the other hand, we expect that the relative coincidence probabilities (i.e. between different baselines and different orientations) are well-represented by the relative mean coincidence probabilities. This should be borne in mind when reading the next two sections and studying Figs 11 and 12.

4.3 COINCIDENCES FOR BURSTS FROM VIRGO

In Fig. 11(a–f) we plot contours of constant $\langle X_1X_2\rangle$ for a number of interesting cases where the source of the waves is the Virgo cluster. We fix the locations of two detectors and plot $\langle X_1X_2\rangle$ as a function of their orientations α_1 and α_2. (Recall that α is the angle between the antenna's bisector and the local east direction. Thus, a '+' orientation is $\alpha=45°$ and a '×' is 90°.) Because of the quadrupole nature of the detector, we need only have plotted the figures for $0°<\alpha<90°$, but we have gone up to 180° for clarity. Maxima in these plots are optimum orientations for coincidences. Although, as we have remarked, we have calculated $\langle X_1X_2\rangle$ analytically, we do not reproduce it here because of its complexity. Any reader who wants a computer printout of it may obtain one by writing to the first author (BFS).

Because there are so many independent variables in $\langle X_1X_2\rangle$, we have had to specify some to get understandable plots. In doing this we have been guided by the principal detectors currently being developed. Thus we have explored baselines among Nevada, Maine, Scotland, and southern Germany. The figures do not change much if a detector is moved a few degrees, such as from Nevada to southern California. The six figures, 11(a–f), describe the six independent baselines among these four sites. The figures assume detectors with perpendicular arms, $2\Omega_1=2\Omega_2=90°$. The more general case can be obtained simply by multiplying the contour values by $\sin^2 2\Omega_1 \sin^2 2\Omega_2$. (This is why we have used the bisector to specify the orientation α. Measuring α from one of the arms would make the transformation of Fig. 11 to the general case more involved.)

Fig. 11(a) refers to detectors in Las Vegas, Nevada (α_1) and Cherryfield, Maine (α_2). The maximum mean coincidence probability is about 5 per cent, for $\alpha_1=75°$, $\alpha_2=50°$, but any pair satisfying $\alpha_2=\alpha_1-22°\pm6°$ gives $\langle X_1X_2\rangle>4.5$ per cent. The most likely value of α_2 seems to be 72° (dictated by geography) for which the optimum value of α_1 is about 4°, i.e. basically a '×' orientation. If α_1 is 20° away from optimum the mean coincidence probability falls by about a quarter. In the worst case, with α_1 as much as 45° from optimum, the coincidence probability is below 2 per cent, a drop of more than half. Remember from our discussion in the last section that the coincidence probabilities should be scaled upwards by a factor of 3 to make them more realistic. This means we can expect roughly one event in six from the Virgo Cluster to register on

both detectors if its amplitude is twice the threshold and if the two detectors are optimally orientated.

Fig. 11(b) is analogous to Fig. 11(a) but for detector 1 in Las Vegas and detector 2 in Glasgow. If the Las Vegas detector has $\alpha_1=4°$ in order to get the best alignment with Cherryfield, then the best value of α_2 is 20°, where $\langle X_1X_2\rangle=2.6$ per cent. This is in fact the largest value of $\langle X_1X_2\rangle$ in the diagram. If α_2 is 45° (a '+' orientation) then this falls to about 2.2 per cent. These values are substantially smaller than for the Maine–Nevada baseline: for sources in Virgo, coincidences between Nevada and Scotland are perhaps half as likely. As a rule of thumb, we can infer from the figure that the best value of α_2 for a given α_1 is $\alpha_2\simeq(\alpha_1+5°)$ for $-5°\leqslant\alpha_1\leqslant40°$ and $\alpha_2\simeq2(\alpha_1-40°)$ for $40°\leqslant\alpha_1\leqslant85°$. This relation has a slope of 2, in marked contrast to the relation for all the other pairs of detectors. This presumably is due to the fact that the planes containing these two detectors are very nearly orthogonal, but it also has to do with their orientation relative to Virgo, since Fig. 12(b) does not show this.

Fig. 11(c) refers to the Las Vegas–Munich baseline. Here the best orientation for Munich is $\alpha_2=10°$ if $\alpha_1=4°$, and the value of $\langle X_1X_2\rangle$ is about 3.2 per cent, a bit higher than for Glasgow–Las Vegas and again optimum over the whole diagram. Significantly, given α_1 the optimum α_2 is $\alpha_2\simeq100°-\alpha_1$, a line of the opposite slope to those in the previous two figures. This is because these detectors are a bit more than 90° apart on a great circle, so a rotation of one is compensated by a rotation of the other in the opposite sense. (Consider two detectors on opposite ends of the Earth diameter.)

Fig. 11(d) is for the baseline from Maine (α_1) to Scotland (α_2). These detectors are relatively close, so the line of optimum alignments is again of slope 1, $\alpha_2\simeq\alpha_1-35°$. If we again take $\alpha_1=72°$ then the best value of α_2 is between 30° and 35°, where $\langle X_1X_2\rangle=2.8$ per cent, nearly the maximum over the whole diagram. This is not far from the optimum Glasgow orientation for Las Vegas, which we saw was 20°. A compromise value of 25° would make the three detectors nearly mutually optimal.

Fig. 11(e) refers to the Maine–Munich baseline, with Munich as detector 2. Again we have a line of optimum angles with a slope of 1, $\alpha_2\simeq\alpha_1-45°$. If $\alpha_1=72°$ then the best value for α_2 is about 25°, giving $\langle X_1X_2\rangle=2.9$ per cent. If Munich is orientated at 10° to give the best coincidence rate with Las Vegas, then this value falls to 2.4 per cent. A value of $\alpha_2=15°$ seems a good compromise, again making the triplet Las Vegas–Maine–Munich mutually optimum.

Finally, Fig. 11(f) treats the European baseline, Glasgow (α_1) to Munich (α_2). Not surprisingly, for such close detectors all the contours have a slope nearly equal to 1, with an optimum $\alpha_2\simeq\alpha_1-10°$. The optimum value is, however, only about 3.5 per cent. This is low compared to the American baseline, Fig. 11(a), not because the detectors do not overlap well, but because at European latitudes the detection rate for events from Virgo is lower than at American latitudes. It is interesting, however, that the orientations of these two detectors that are optimum for coincidences with the American ones, $\alpha_1=25°$ and $\alpha_2=15°$, are optimum here as well. It is therefore possible to orient all four detectors in such a way that they are mutually optimum for coincidences.

In a future paper we will investigate what this implies for the double, triple, and quadruple coincidence rates.

4.4 COINCIDENCES FOR ISOTROPICALLY DISTRIBUTED BURST SOURCES

In Fig. 12 (a–f) we draw contours of constant

$$\langle X_1X_2\rangle_\theta=\frac{1}{2}\int_0^\pi\langle X_1X_2\rangle\sin\theta\,d\theta, \tag{4.9}$$

which is the mean coincidence rate for sources isotropically distributed over the sky. The figures treat the baselines in the same order as Fig. 11(a–f). The maximum probabilities are higher here, by more than a factor of 2 for the European baseline. Given that the Maine detector is at 72°, the best orientations of the others may be deduced from the figures: Las Vegas, 12°; Glasgow, 10°; Munich, 0°. These are again a set of orientations which are nearly optimum for all baselines. They give mean coincidence probabilities for the various baselines as follows: Maine–Nevada, 6.5 per cent; Nevada–Glasgow, 4.4 per cent; Nevada–Munich, 4.1 per cent; Maine–Glasgow, 5.8 per cent; Maine–Munich, 5.2 per cent; Glasgow–Munich, 8 per cent. The transAtlantic baselines and especially the European baseline have much improved coincidence rates for isotropic sources. But the orientations that are best here are not the same as for sources in Virgo. If there is flexibility in orientating the detectors on the sites that are eventually chosen, the choice of orientation may depend upon which type of source is regarded as most likely.

5 Conclusions

Our principal theoretical result is the proof of (4.8), that the threshold averaged coincidence probability for two detectors equals the mean of the product of their antenna power patterns. This allows one to use threshold-independent criteria for judging the likelihood of coincidences between detectors. The figures we have prepared contain considerable information of use both in planning detectors and in interpreting observations. They raise a number of questions about the choice of orientations and the strategy regarding coincidence observations. We shall just make a few remarks on these questions here. It is too early to draw firm conclusions.

If, as our calculations suggest, the coincidence rates for marginal events (twice the amplitude threshold) are between 10 and 15 per cent for sources in Virgo, and between 20 and 30 per cent for isotropically distributed sources, then it is clear that two detectors in America, say, will miss a substantial fraction of the events. If only one other detector is built in Europe, then the orientation ought to be chosen to maximize coincidences with the American ones, since mutually optimum orientations are available. But if two detectors are built in Europe, two different strategies are possible: they can be orientated either to maximize coincidences with the American ones and with each other or to minimize transAtlantic coincidences while maximizing European ones.

The motivation for this second strategy, which we shall call 'complementarity', is to catch some of the events that the American detectors miss. How many events would be caught this way cannot be deduced from our present calculations, since it depends on the thresholds. But it is conceivable that the network as a whole could detect twice as many events as the American baseline alone would see. More than this seems unlikely in view of the intrinsically lower coincidence rate of the European baseline.

The advantages of the first strategy, of aligning all detectors mutually optimally ('supplementarity'), are that it (i) enhances transAtlantic double coincidences, and (ii) presumably enhances the rates of triple and quadruple coincidences. The extra transAtlantic doubles may make up in part for the ones lost by not adopting complementarity. But its principal and possibly decisive advantage is in the importance of triple coincidences. Since the two European detectors would be relatively close together, they should see mostly the same events. So a transAtlantic double coincidence is very likely to be a triple, and a coincidence involving both American detectors and at least one European one would also very likely turn out to be a quadrupole.

Triple coincidences are desirable for two main reasons. First, they give added confidence that an event has occurred. If events are not otherwise corroborated (such as by the subsequent visual detection of a supernova), this could be crucial. It is conceivable that there are large gravitational

wave events which are not accompanied by large electromagnetic emissions, and triple coincidences would be helpful in their identification. The second reason is that one can get much more useful information from a triple observation: two independent time-delay observations pinpoint the source on the sky, and the three amplitude observations contain redundant information for determining h and the polarization ψ. This redundancy would allow a test of general relativity, such as of the transverse nature of the polarization or the speed of the wave. Triple coincidences are therefore much more desirable than doubles.

The importance of triples, plus the fact that any three detectors are unlikely, by the present calculations, to have a triple rate of higher than 20 per cent for $X_*=0.25$, means that it is very important that there be at least four detectors world-wide. Four detectors have four independent triplets, which must enhance the triple coincidence rate by something like at least a factor of 2. Further detectors are also highly desirable. In this regard it is heartening that a group in France has begun to make plans for a detector. A further detector widely separated from the others, such as in Asia or the Southern Hemisphere, could make a significant increase in the sensitivity of the network as a whole.

The rates of triples and the fraction of all events that a given network of detectors will see cannot be inferred accurately from the present calculations. We are currently calculating actual coincidence rates (doubles and triples) as functions of the thresholds of the detectors in various orientations, among them the preferred orientations determined by the present paper. Without limiting the orientation freedom in some way, coincidence-rate calculations have too many independent variables to be tractable. In that sense, the present calculations are a natural precursor to the full coincidence-probability calculations we shall publish subsequently.

Acknowledgments

We thank Ron Drever, Jim Hough and Albrecht Rüdiger for very helpful comments on an earlier version of this paper. Massimo Tinto acknowledges the support of the Italian Ministry of Education.

References

Drever, R. W. P., 1982. In: *Gravitational Radiation,* eds Deruelle, N. & Piran, T., North Holland, Amsterdam.
Estabrook, F. B., 1985. *Gen. Rel. Grav.,* **17,** 719.
Forward, R. L., 1978. *Phys. Rev. D,* **17,** 379.
Goldstein, H., 1965. *Classical Mechanics,* Addison-Wesley, New York.
Maischberger, K., Rüdiger, A., Schilling, R., Schnupp, L., Shoemaker, D. & Winkler, W., 1985. *Vorschlag zum Bau eines grossen Laser-Interferometers zur Messung con Gravitationswellen,* MPQ 96, Max-Planck-Inst. für Quantenoptik, Garching.
Misner, C. W., Thorne, K. S. & Wheeler, J. A., 1973. *Gravitation,* W. H. Freeman & Co., San Francisco.
Schutz, B. F., 1985. *A First Course in General Relativity,* Cambridge University Press.
Weiss, R., In: *Sources of Gravitational Radiation,* ed. Smarr, L., Cambridge University Press.